Theor Chem Acc (2005) 114: 242–252
DOI 10.1007/s00214-005-0667-7

REGULAR ARTICLE

D. J. Simpson · T. Bredow · A. R. Gerson

# MSINDO study of water adsorption on NiO surfaces

Received: 6 July 2004 / Accepted: 15 February 2005 / Published online: 7 July 2005


**Abstract** The dissociation of water adsorbed on the surface of NiO was investigated by using the semi-empirical SCF MO method MSINDO. Simulations were based on embedded cluster models representing the (100) surface, with and without a monatomic step. The angle formed between the metal adsorption site and the O–H bond associated with water has been found to be critical to the energetics of the dissociation process. Based on this criterion, it was shown that water dissociation is favorable on the stepped surface, but highly unlikely on the planar surface. In addition, the activation energy required for water dissociation in a monatomic NiO step was considerably lower than for dissociation at the planar surface. The high activation energy associated with water dissociation on the planar surface is attributed to the rigidity of the NiO lattice.

**Keywords** Nickel oxide · Water adsorption · Semiempirical methods and calculations · Dissociation · Geometrical criteria · Activation energy

## 1 Introduction

On dissolution in an aqueous medium, solids undergo a range of chemical reactions. Water plays an important role in the dissolution, not only as a transport agent for dissolved components, but also as a reactant [1]. Water adsorption onto planar surfaces of MgO has been frequently studied, yet the debate between molecular versus dissociative adsorption still creates much controversy [2]. Less controversial is the adsorption of water on the planar NiO(100) surface although the investigation of this system to date is limited to experimental approaches. A thorough search through the literature did not reveal any article claiming water dissociation on the planar surface. However, water dissociation has been noted on defective NiO surfaces [3–6].

In a previous theoretical study [7], we have shown that dissolution can initiate at the perfect planar MgO(100) surface. MgO is unstable in low pH solution and dissolves readily at room temperature. The most favorable initial dissolution pathway involved the formation of square pits via restructuring of the protonated surface. This process relies on the dissociation of water molecules at the planar surface. Furthermore, a molecular dynamics study by de Leeuw and Parker [8] has shown that the MgO(100) surface is unstable in liquid water. In contrast to highly reactive MgO surfaces, the measured dissolution rate of NiO is several orders of magnitude smaller [9] under the same conditions. In addition, the NiO surface does not appear to reconstruct at the outset of dissolution [10]. Ludwig and Casey [11] proposed that dissolution may start at a roughened NiO(111) surface. However, we cannot find any reports of dissolution initiating from the planar NiO(100) surface.

The reactivity of NiO is, however, more sensitive than MgO to preparation conditions. Jones et al. [12] and Pease et al. [13] reported a strong dissolution rate dependence on annealing temperature. It appears that the removal of water (i.e. dehydration) decreases the reactivity of NiO. According to Parks [14], the incorporation of water into the bulk structure (i.e. hydrated oxide) alters the surface properties and reactivity in solution.

For the purpose of the present study, we only consider the anhydrous form of NiO. Crystalline NiO is face-centerd-cubic (fcc) and is isostructural with MgO and NaCl. The most stable surface of these fcc crystals is the (100) lattice plane.

Aqueous dissolution is a complex process and therefore there is no doubt that several factors control the dissolution kinetics of oxide minerals in solution. One of them is the

Dedicated to Prof. K. Jug in honor of his 65th birthday

D. J. Simpson
Ian Wark Research Institute, University of South Australia, Mawson Lakes, Adelaide, SA 5095, Australia

T. Bredow
Theoretische Chemie, Universität Hannover, Am Kleinen Felde 30, 30167 Hannover, Germany

A. R. Gerson (✉)
Applied Centre for Structural and Synchrotron Studies, University of South Australia, Mawson Lakes, SA 5095, Australia
E-mail: andrea.gerson@unisa.edu.au

activation energy for the dissociation of adsorbed water. According to Henderson [2], water dissociation can reveal information as to the reactivity of a surface towards other chemical processes. The purpose of the present study was to determine if there are any significant differences in the activation energy and structures resulting from water dissociation between the planar and the stepped surfaces using quantum chemical calculations. The results for NiO were compared to those for MgO obtained with the same method.

## 2 Method of calculation

The semiempirical SCF MO method MSINDO is based on the ZDO approximation [15, 16]. Only one- and two-center interaction integrals are evaluated, thus reducing the total number of integrals for a $N$-electron system to $N^2$ compared to $N^4$ in the case of ab initio Hartree-Fock (HF) methods or $N^3$ for density-functional theory (DFT) based methods. This enables the investigation of relatively large and complex systems with low symmetry and hundreds of atoms. In order to compensate for the neglect of interaction integrals, empirical parameters are introduced in MSINDO, replacing the analytical calculation of one-electron two-center integrals [17]. In semiempirical methods only valence electrons are treated explicitly. For Ni atoms, the 10 electrons of the 4s3d valence shell, and for O atoms the 6 electrons of the 2s2p valence shell are taken into account. Contributions of inner electrons are described by Zerner's pseudopotential [18].

The present parameter set [18] was optimized using results from B3LYP calculations of $(NiO)_n$ clusters with $n = 2$ and 4, representing small units of the NiO lattice as well as experimental data from gas phase molecules. In this way, it is possible to describe with comparable accuracy gas phase molecules containing nickel atoms, and NiO bulk and surface properties [18, 19] using the same set of parameters. As demonstrated earlier [17], geometrical and thermodynamic data of oxygen and hydrogen containing molecules calculated with MSINDO are also in reasonable agreement with the literature. Therefore the adsorption studies presented here can be expected to be qualitatively and even semi-quantitatively correct. Geometry optimisation in MSINDO is based on the Newton-Raphson method [20, 21]. The transition-state structure used to estimate the activation energy was derived by full-force constant matrix calculations using the Cartesian coordinates of selected atoms. Since the transition state calculation takes much longer than geometry optimization, only a minimum number of atoms were selected. The energy threshold for the SCF procedure was set at a moderately accurate value, $1 \times 10^{-6}$ Hartree, in order to further reduce the computational effort.

Two-dimensional periodic structures (slab models) provide a more accurate description of long-range Coulomb interactions than cluster models. However, cluster models are more appropriate for describing local effects, such as the formation of surface defects. Periodic approaches require large super-cells to prevent defect interaction and therefore are computationally costly. In MSINDO, an embedding procedure has been introduced that describes the long-range Coulomb interactions of the ionic environment and also approximates short-range interactions of the cluster's surroundings, in order to minimize boundary effects [22].

Bulk and surface properties of NiO calculated with MSINDO, were reported in a study by Bredow et al. [19]. Models based on the cyclic cluster approach were compared to free and embedded clusters. The calculated unit cell parameter and heat of atomization agreed well with accurate experimental data. The experimental band gap, 3.8 eV, is overestimated, but the MSINDO result (6.8–7.0 eV) is still an improvement to HF derived values since semiempirical methods mimic the inclusion of electron correlation, which is absent in pure HF calculations. Surface properties namely relaxation, rumpling and relaxation energy were also derived for the different models. The properties calculated for the cyclic and embedded models in particular agree well with the experimental values.

The adsorption energy calculated using the original MSINDO method for molecular water at low coverage on MgO(100) agrees well with the best experimental value at zero coverage [23]. However, the dissociated form of water was found to be overly stable as compared to the molecular form [24], in contradiction to previous high-level calculations. Therefore, an empirical correction for the O–H bond in MSINDO was introduced in the previous MgO study [7]. Consequently, the adsorption energies for dissociated water on MgO are comparable to values from high accuracy studies. The same correction was used in this study on NiO.

In the present calculations the electronic structure of NiO is simplified. Instead of the antiferromagnetic $AF_2$ ground state a ferromagnetic state was considered. In earlier MSINDO investigations it was found that the energetic difference between antiferromagnetic and ferromagnetic states is small, in agreement with experiment [19]. It was assumed that every Ni ion has a $s^0d^8$ configuration with two unpaired electrons in the d shell. Therefore, the multiplicity of the $Ni_{128}O_{128}$ cluster is 257. This state was treated with the unrestricted HF method.

## 3 Planar surface

A stoichiometric neutral $Ni_{128}O_{128}$ cluster embedded in a finite array of pseudo atoms was used as the model for the planar surface region. The central 256 atoms were arranged in an $8 \times 8 \times 4$ quadratic block (representing 8 atoms in the $x$- and $y$-directions, and 4 atoms in the $z$-direction). The cluster shown in Fig. 1 is surrounded by two layers of pseudo atoms in the $\pm x$, $\pm y$ and $-z$ directions, resulting in an overall $12 \times 12 \times 6$ arrangement. The surface size was chosen to be as large as possible (within the limitations of available computer resources) in order to minimize boundary effects for the innermost surface atoms.

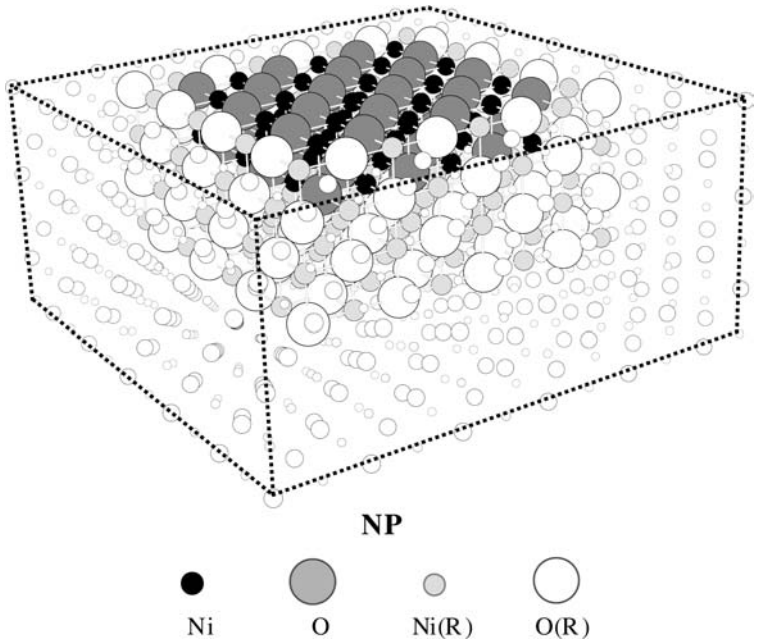


**Fig. 1** The embedded 8×8×4 NiO cluster with 6×6×2 relaxation (NP) representing the planar surface region: relaxed nickel and oxygen atoms are denoted Ni and O, respectively while fixed nickel and oxygen atoms are denoted Ni(R) and O(R), respectively

### 3.1 Models with 6 × 6 × 2 relaxation

Surface relaxation energies determined previously by MSINDO calculations on MgO were much closer to high accuracy calculations if only the inner 6 × 6 × 2 atoms were relaxed rather than all the atoms of the top 8×8×2 layers [25]. Therefore, the relaxed planar model (NP) shown in Fig. 1 involves optimization of the inner 6×6 surface atoms and the inner 6×6 atoms of the second layer while the remaining atoms were fixed at their bulk positions.

In Fig. 2, models representing molecular and dissociated water adsorption on the relaxed 6 × 6 × 2 surface are denoted $NP_{MOL}$ and $NP_{DIS}$, respectively. For molecular adsorption, the parallel configuration is shown. Although this is not as stable as the tilted structure, the difference between these configurations is only 6 kJ mol$^{-1}$ according to a similar study on MgO(100) by Tikhomirov and Jug [26]. The oxygen atom of the water molecule binds to a metal site while the hydrogen atoms of the water molecule hydrogen bond to lattice oxygen sites separated by 90° about the nickel site. This orientation has also been reported in theoretical studies of water on planar MgO(100) [24, 27, 28].

From a molecular dynamics study of water adsorption on the MgO surface, Langel and Parrinello [29] proposed a set of criteria for water dissociation. According to Langel and Parrinello [29], the strength of the hydrogen bond from water to lattice oxygen sites is characterized by the distance between the oxygen atom of the hydroxyl group and the oxygen adsorption site (referred to as $R_{O..O}$ distance) together with the angle formed by the hydroxyl group relative to the hydrogen bond, given as $\Phi_{O–H..O}$ [29]. A short $R_{O..O}$ distance and a $\Phi_{O–H..O}$ angle close to 180° corresponds to a strong hydrogen bond. The angle defined by the M–O bond between water and the metal site with the dissociating O–H bond was defined as $\Phi_{Mg–O–H}$. It was suggested by Langel and Parrinello [29] that the $\Phi_{Mg–O–H}$ angles play a crucial role in the enhanced chemical activity of the step defect and cannot be exclusively attributed to oxygen atoms of reduced coordination. Consequently, structures and reaction pathways, which include $\Phi_{Mg–O–H}$ angles lower than about 90° seem to be highly improbable.

Due to the lack of reference data for NiO, geometrical parameters and adsorption energies for the NiO system are compared to MgO calculations obtained with MSINDO. Adjacent to the ball and stick models shown in the figures are lines for selected bond angles and distances. For the purpose of this study, we prefer to use the $\Phi_{O\sim H\sim O}$ notation to indicate that the H-atom is transferred from the O-atom of water to a lattice O-site. Instead of the $\Phi_{Mg–O–H}$ notation, we use $\Phi_{Ni–O\sim H}$ to indicate that the OH bond is broken during dissociation (for NiO). In addition, we also consider the bond length between the metal adsorption site and the oxygen atom associated with water or the OH fragment ($R_{Ni–OH}$). The distance between the hydrogen fragment of water and the designated oxygen adsorption site is denoted $R_{NiO\sim H}$. The bond distance between the metal and oxygen adsorption sites, i.e. the bond in line with the dissociating O–H bond, is denoted $R_{Ni–O}$. The bond length of the dissociating O–H bond in water is designated $R_{O\sim H}$. The H–O–H bond angle of water, and the angle defined by the dissociating O–H bond relative to the newly formed O–H bond are denoted as $\Phi_{H–O\sim H}$ and $\Phi_{O\sim H\sim O}$, respectively. The geometrical parameters shown in

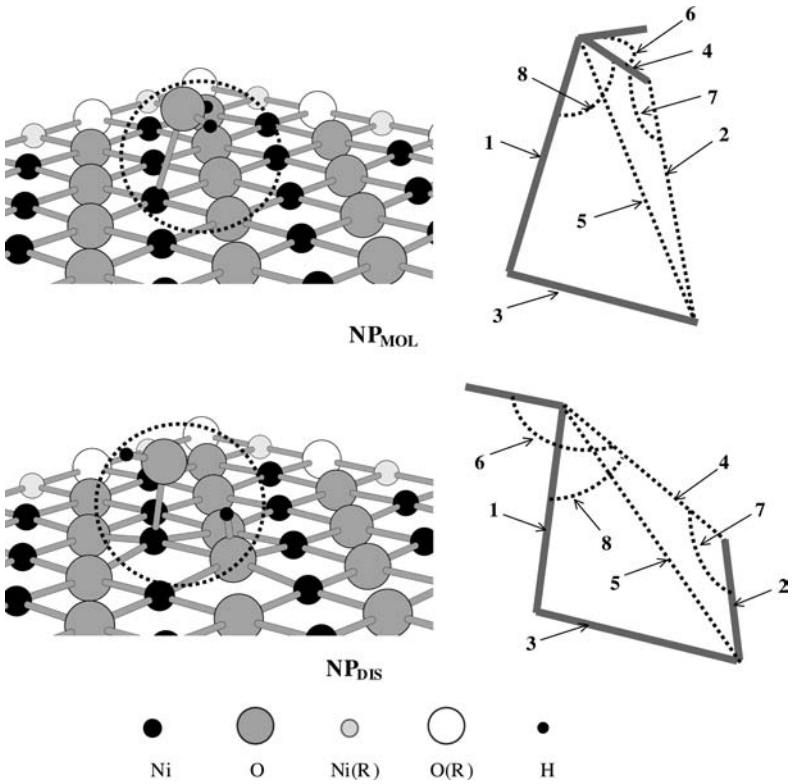


**Fig. 2** Molecular and dissociative adsorption for single water molecule on the planar NiO surface with 6×6×2 relaxation; selected distances and bond angles highlighted by lines are labeled 1–8: (1) $R_{Ni-OH}$, (2) $R_{NiO\sim H}$, (3) $R_{Ni-O}$, (4) $R_{O\sim H}$, (5) $R_{O\cdot\cdot O}$, (6) $\Phi_{H-O\sim H}$, (7) $\Phi_{O\sim H\sim O}$ and (8) $\Phi_{Ni-O\sim H}$

Fig. 2, namely $R_{Ni-OH}$, $R_{NiO\sim H}$, $R_{Ni-O}$, $R_{O\sim H}$, $R_{O\cdot\cdot O}$, $\Phi_{H-O\sim H}$, $\Phi_{O\sim H\sim O}$ and $\Phi_{Ni-O\sim H}$, are labeled 1–8, respectively.

For molecular adsorption on the planar MgO surface, Langel and Parinello [29] reported the parameters $R_{O\cdot\cdot O}$ (label 5) and $\Phi_{O\sim H\sim O}$ (label 7) as 2.60 Å and 160°, respectively. In comparison, the corresponding values in Table 1 for NiO are 2.68 Å and 123°, respectively. This would suggest that the hydrogen bond between water and the NiO surface is not as strong as for MgO. However, for a method-consistent comparison, these values need to be compared to MSINDO results for MgO [30]. Shown in parenthesis, the corresponding values for MgO are 2.65 Å and 126°, respectively. Therefore, according to MSINDO calculations, hydrogen bonding is equally strong for both oxides. For $\Phi_{Ni-O\sim H}$ (label 8, or $\Phi_{Mg-O\sim H}$ in the case of MgO), Langel and Parrinello calculated 80° for the planar MgO surface. Since this value is below the 90° threshold, it would indicate that dissociation is not favorable. In contrast, the 95° calculated with MSINDO would suggest that dissociation is likely to initiate on the planar MgO surface. For planar NiO, the $\Phi_{Ni-O\sim H}$ value at 89° would indicate that dissociation is a slightly unfavorable pathway. The remaining $NP_{MOL}$ geometry parameters have similar values as for the corresponding MgO model except for $R_{Ni-O}$ (label 3, or $R_{Mg-O}$ in the MgO case) [30]. The $R_{Ni-O}$ value shown in Table 1 for the dry surface (NP) is 2.06 Å. The 2.13 Å value for $NP_{MOL}$ indicates a 3% increase in this bond length due to molecular adsorption. For MgO, molecular adsorption increases the corresponding bond length considerably more, by 11% [30].

The $R_{O\cdot\cdot O}$ and $\Phi_{O\sim H\sim O}$ values (labels 5, 7, respectively) of the dissociative model $NP_{DIS}$ are similar to corresponding values of the $NP_{MOL}$ model. This would indicate that hydrogen bonding associated with the $NP_{DIS}$ model is of equal strength to the $NP_{MOL}$ model. This result was also obtained for the corresponding MgO models [30]. The $\Phi_{Ni-O\sim H}$ value (label 8) for $NP_{DIS}$ with 76° is significantly lower than the 90° threshold. Therefore, the decrease in this parameter with respect to the $NP_{MOL}$ value indicates an unfavorable reaction pathway. For MgO, the $\Phi_{Mg-O\sim H}$ value also decreases in the dissociative adsorption structure compared to the molecular form, however, it was still close to 90°. Therefore dissociation on the planar MgO surface would appear to be a borderline case. However, Langel and Parrinello [29] also calculated $\Phi_{Mg-O\sim H} = 90°$ for the dissociated structure in the MgO step and concluded that dissociation was favorable. The proposed transfer of the hydrogen fragment from water to the NiO surface can be seen by the different values of $R_{NiO\sim H}$ and $R_{O\sim H}$ (labels 2 and 4, respectively) for $NP_{MOL}$ and $NP_{DIS}$. With respect to the dry surface, dissociative adsorption on NiO increases the distance between the adsorption sites ($R_{Ni-O}$, label 3) by 11%. This value is significantly larger than the value for molecular adsorption. For MgO, dissociative adsorption increases the corresponding metal-oxygen bond by a considerable 25%. Therefore, dissociative adsorption is more

**Table 1** Calculated bond lengths $R_{Ni–OH}$, $R_{NiO\sim H}$, $R_{Ni–O}$, $R_{O\sim H}$ and $R_{O\cdot\cdot O}$ (Å), and bond angles $\Phi_{H–\cdot\cdot O\sim H}$, $\Phi_{O\sim H\sim O}$ and $\Phi_{Ni–O\sim H}$ (degrees) for molecular and dissociated structures based on NP model with 6×6×2 relaxation (as shown in Fig. 2). Adsorption energies are denoted by $E_{ads}$ (kJ mol$^{-1}$); see Eq. (1). Results based on equivalent MgO models in parenthesis [30]

| Model | Label No. | NP | $NP_{MOL}$ | $NP_{DIS}$ |
|---|---|---|---|---|
| $R_{Ni–OH}$ | 1 | | 2.16 | 1.86 |
| $R_{NiO\sim H}$ | 2 | | 2.02 | 0.97 |
| $R_{Ni–O}$ | 3 | 2.06 (2.16) | 2.13 (2.39) | 2.29 (2.69) |
| $R_{O\sim H}$ | 4 | | 0.97 | 1.97 |
| $R_{O\cdot\cdot O}$ | 5 | | 2.68 (2.65) | 2.65 (2.53) |
| $\Phi_{H–O\sim H}$ | 6 | | 107 | 112 |
| $\Phi_{O\sim H\sim O}$ | 7 | | 123 (126) | 125 (130) |
| $\Phi_{Ni–O\sim H}$ | 8 | | 89 (95) | 76 (90) |
| $E_{ads}$ | | | −55 (−31) | −53 (−38) |

effective in weakening the bond between the adsorption sites than molecular adsorption. This effect is considerably more pronounced for MgO than for NiO.

Based on Eq. 1, the adsorption energy was calculated with respect to gas phase water.

$$Ni_{128}O_{128} + H_2O \rightarrow [Ni_{128}O_{128} : H_2O] \quad (1)$$

The adsorption energies for molecular and dissociative adsorption of a single water molecule with 6×6×2 surface relaxation are −55 and −53 kJ mol$^{-1}$, respectively (Table 1). The corresponding values for MgO are −31 and −38 kJ mol$^{-1}$, respectively [10]. Therefore water adsorption on the planar NiO surface is significantly more exothermic than on MgO. In an experimental study, the desorption energy of water on NiO(100) was reported as 45 kJ mol$^{-1}$ [31]. This is quite similar to the calculated value. However, it has to be taken into account that adsorption and desorption involve different reaction steps. A comparison of calculated adsorption energies and measured desorption energies is therefore not straightforward.

### 3.2 Models with 2×2×1 relaxation

For the transition state search the number of surface atoms included in the geometry optimization had to be reduced. From previous calculations of the $H_2O$/MgO(100) system, it was found that a 2×2×1 surface dimensions still gives a reasonable approximation to results obtained with the larger 6×6×2 relaxation dimensions [10].

The models with restricted 2×2×1 surface optimization representing molecular and dissociated adsorption in Fig. 3 are denoted $NP_{MOL}$(R) and $NP_{DIS}$(R), respectively. In addition, the transition state structure with restricted surface optimization is denoted $NP_{TS}$(R). The activation energy is defined as the difference in the adsorption energy values between the TS and MOL structures, with the same restricted surface relaxation.

The geometry parameters listed in Table 2 for the molecular and dissociative cases with 2×2×1 relaxation are very close to their corresponding values obtained with the more extended 6×6×2 relaxation (Table 1). The largest difference between the two optimization strategies is obtained for the adsorption energy in the case of dissociative adsorption. With 2×2×1 relaxation, dissociative adsorption is 46 kJ mol$^{-1}$ higher in energy compared to the 6×6×2 relaxation. Further discussion on this effect is presented in the next section.

Interestingly, the $R_{Ni–O}$ bond length for the transition state structure is close to the dry surface value (Table 2). Sharing of the hydrogen fragment between OH from water and hydrogen-bonded oxygen surface site in model $NP_{TS}$(R) creates intermediate bond lengths $R_{NiO\sim H}$ and $R_{O\sim H}$ (labels 2 and 4, respectively). Compared to the molecular and dissociative models, the transition state structure has a shorter $R_{O\cdot\cdot O}$ distance (label 5) and a larger $\Phi_{O\sim H\sim O}$ angle (label 7). Thus, water is more strongly hydrogen bonded with the surface at this stage of the dissociation process. However, the $\Phi_{Ni–O\sim H}$ (label 8) value of $NP_{TS}$(R) is significantly smaller than the molecular and dissociated cases. This value is well below the 90° threshold of Langel and Parrinello [29]. The rigidity of the NiO surface forces the $\Phi_{Ni–O\sim H}$ to adopt a low value of 64°. Since this configuration is unstable, a large activation energy of +198 kJ mol$^{-1}$ is obtained. There is no doubt from this result that water dissociation on the planar NiO(100) is highly improbable.

For dissociation on planar MgO(100), a smaller activation energy of +72 kJ mol$^{-1}$ was calculated [30]. This has to be compared to the +30 kJ mol$^{-1}$ energy barrier calculated by Ahlswede et al. [24] with MSINDO. This difference is caused by two factors. One is the degree of relaxation and the other is the empirical correction factored into MSINDO for this study. For comparison, additional calculations show that a smaller 2×1×1 relaxation increases the activation energy to +96 kJ mol$^{-1}$ [10]. Therefore, the activation energy increases with reduced relaxation dimensions. From previous work, the activation energy for dissociation on the planar MgO surface with multiple adsorbed water molecules and protons was +70 kJ mol$^{-1}$ [7]. Therefore, the effect of these additional species on the activation energy does not appear to be significant.

### 3.3 The effect of relaxation dimensions on adsorption energy

A series of calculations were carried out examining the adsorption of a single water molecule at a central site of the

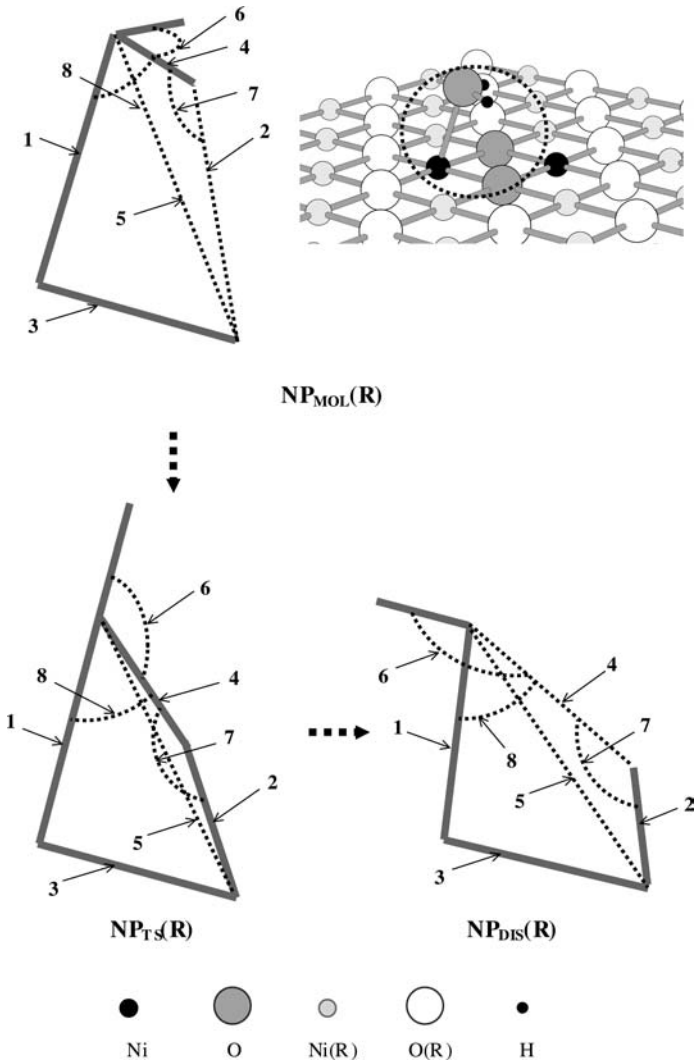


**Fig. 3** Adsorption of a single water molecule on the planar NiO surface with 2×2×1 relaxation for molecular, transition state and dissociative configurations: selected distances and bond angles highlighted by lines: (1) $R_{\mathrm{Ni-OH}}$, (2) $R_{\mathrm{NiO\sim H}}$, (3) $R_{\mathrm{Ni-O}}$, (4) $R_{\mathrm{O\sim H}}$, (5) $R_{\mathrm{O\cdot\cdot O}}$, (6) $\Phi_{\mathrm{H-O\sim H}}$, (7) $\Phi_{\mathrm{O\sim H\sim O}}$ and (8) $\Phi_{\mathrm{Ni-O\sim H}}$

**Table 2** Calculated bond lengths $R_{\mathrm{Ni-OH}}$, $R_{\mathrm{NiO\sim H}}$, $R_{\mathrm{Ni-O}}$, $R_{\mathrm{O\sim H}}$ and $R_{\mathrm{O\cdot\cdot O}}$ (Å), and bond angles $\Phi_{\mathrm{H-O\sim H}}$, $\Phi_{\mathrm{O\sim H\sim O}}$ and $\Phi_{\mathrm{Ni-O\sim H}}$ (degrees) for molecular, transition state and dissociated structures based on the NP model with 2×2×1 relaxation (as shown in Fig. 3). Adsorption energies are denoted by $E_{\mathrm{ads}}$ (kJ mol$^{-1}$); see Eq. (1). Results based on equivalent MgO models in parenthesis [30]

| Model | Label No. | NP(R) | $NP_{MOL}(R)$ | $NP_{TS}(R)$ | $NP_{DIS}(R)$ |
|---|---|---|---|---|---|
| $R_{\mathrm{Ni-OH}}$ | 1 | | 2.16 | 2.10 | 1.87 |
| $R_{\mathrm{NiO\sim H}}$ | 2 | | 2.04 | 1.28 | 0.98 |
| $R_{\mathrm{Ni-O}}$ | 3 | 2.05 (2.16) | 2.10 (2.27) | 2.07 (2.38) | 2.22 (2.47) |
| $R_{\mathrm{O\sim H}}$ | 4 | | 0.97 | 1.21 | 1.93 |
| $R_{\mathrm{O\cdot\cdot O}}$ | 5 | | 2.68 (2.66) | 2.45 (2.33) | 2.61 (2.53) |
| $\Phi_{\mathrm{H-O\sim H}}$ | 6 | | 107 | 113 | 114 |
| $\Phi_{\mathrm{O\sim H\sim O}}$ | 7 | | 122 (122) | 160 (141) | 124 (130) |
| $\Phi_{\mathrm{Ni-O\sim H}}$ | 8 | | 90 (94) | 64 (87) | 75 (82) |
| $E_{\mathrm{ads}}$ | | | −50 (−26) | 148 (46) | −7 (17) |

**Table 3** The effect of relaxation dimensions on adsorption energies $E_{ads}$ (kJ mol$^{-1}$) for one water moiety on the planar surface. Results based on equivalent MgO models in parenthesis [30]

| Relaxation | MOL | DIS | Difference |
|---|---|---|---|
| None | −46 (−27) | 113 (168) | 159 (195) |
| 2×2×1 | −50 (−26) | −7 (17) | 43 (43) |
| 4×4×1 | −49 (−28) | −16 (−24) | 33 (4) |
| 6×6×1 | −51 (−29) | −28 (−24) | 23 (5) |
| 6×6×2 | −55 (−31) | −53 (−38) | 2 (7) |

NiO 8×8×4 cluster. The dependence of adsorption energies on varying degrees of relaxation is shown in Table 3. The minimum relaxation (2×2×1) refers to models $NP_{MOL}(R)$ and $NP_{DIS}(R)$ while models $NP_{MOL}$ and $NP_{DIS}$ represent maximum 6×6×2 relaxation. The calculated molecular adsorption energies shown range from −46 kJ mol$^{-1}$ to −55 kJ mol$^{-1}$, depending on the extent of surface relaxation. Therefore, surface relaxation makes very little difference to the energetics of molecular adsorption. This was also the case for a MgO 8×8×4 cluster as model for MgO(100), where corresponding adsorption energies ranged from −26 kJ mol$^{-1}$ to −31 kJ mol$^{-1}$[10]. For dissociative adsorption on NiO, however, the heat of reaction varies from +113 kJ mol$^{-1}$ to −53 kJ mol$^{-1}$ depending on the degree of relaxation. The corresponding values for MgO range from +168 kJ mol$^{-1}$ to −38 kJ mol$^{-1}$ [10]. This process becomes more exothermic as the degree of relaxation is increased, particularly with the inclusion of second layer atoms. For the dissociative case, there is a clear dependence on the extent of surface relaxation. A similar effect has also been reported previously for water adsorption at anatase (001) [32]. Even 2×2×1 relaxation (involving only four surface atoms) has a dramatic stabilizing effect in the dissociative cases. Also shown in Table 3, are the differences between the molecular and dissociative adsorption energies. As the relaxation dimension increases, the difference diminishes. Therefore, the influence of relaxation dimensions on the energetics must be taken into account.

## 4 Monatomic step

Models of a stoichiometric monatomic step were based on the 8×8×4 cluster with an additional 8×4×1 layer aligned to one side of the cluster with an overall stoichiometry of $Ni_{144}O_{144}$ (Fig. 4). The corresponding monatomic step model used by Ahlswede et al. [24] for MgO was based on an embedded 9×9×3+9×5×1 cluster, with the stoichiometry $Mg_{144}O_{144}$. The cluster shown in Fig. 4 is surrounded by two layers of pseudo atoms in the $\pm x$, $\pm y$ and $-z$ directions, resulting in an overall 12×12×6+12×6×1 arrangement.

### 4.1 Models with 6×6×1+6×3×1 relaxation

For the relaxed model, relaxation was limited to the 6×6×1 atoms of the original surface plus the additional 6×3×1 atoms of the extra layer. The other atoms remained fixed in their bulk positions (Fig. 4).

According to the results of Ahlswede et al. [24], the most stable configuration for molecular adsorption in an MgO step involves one O–H bond lying nearly parallel with the edge of the step while the other O–H bond points out of the step. This orientation was therefore used as the starting point for the optimized structure $NS_{MOL}$ shown in Fig. 5. The water molecule is bound to the four and five fold coordinated sites of the 8 × 8 × 4 + 8 × 4 × 1 model. In contrast, the model used by Langel and Parrinello [29] contained steps with (100) and (010) faces built on the (011) plane. Consequently, water molecules sitting in the step were bound to five fold coordinated sites. For the dissociative model $NS_{DIS}$, bonding to the oxygen atom from OH is also shared between four and five fold coordinated nickel sites (Fig. 5). Dissociative adsorption at the monatomic step induces more distortion of the lattice as compared to molecular adsorption.

As explained for the planar case, the corresponding geometrical parameters have been labeled from 1 to 8. Since the oxygen atom of water (in Fig. 5) is shared between two nickel sites in the monatomic step, there are two values for $\Phi_{Ni-O\sim H}$ (label 8). Two $\Phi_{O\sim H\sim O}$ (label 7) angles are also present for the hydrogen atom shared between two oxygen sites. The two values for each $\Phi_{O\sim H\sim O}$ and $\Phi_{Ni-O\sim H}$ angles were averaged and listed in Tables 4 and 5.

For molecular adsorption in the monatomic NiO step (i.e. $NS_{MOL}$), the hydrogen bond strength parameters $R_{O..O}$ (label 5) and $\Phi_{O\sim H\sim O}$ (label 7) in Table 4 are 2.59 Å and 108°, respectively. Compared to the respective MgO values, 2.76 Å and 106° [30], it appears that water is bound slightly more strongly to the defective NiO surface. In addition, the $R_{Ni-OH}$ (label 1) and $R_{NiO\sim H}$ (label 2) distances are significantly shorter than the equivalent parameters for the corresponding MgO model [30]. The $\Phi_{Ni-O\sim H}$ (label 8) angle of $NS_{MOL}$, 95°, is above the threshold for a favorable reaction pathway. In contrast, the same parameter for the $NP_{MOL}$ model is below the 90° threshold (Table 1). Molecular adsorption increases the $R_{Ni-O}$ value (label 3) of the adsorption site by 7% with respect to the dry surface. For MgO, the equivalent bond length increases by 3% compared to the dry surface [30].

From Table 4, the considerable increase in the $R_{O..O}$ distance (label 5) of model $NS_{DIS}$ (with respect to $NS_{MOL}$) indicates that hydrogen bonding is weaker after dissociation. This hydrogen bond is weakened as a result of the hydration and strengthening of the bond between the dissociated hydrogen fragment and the surface oxygen. Since the 93° $\Phi_{Ni-O\sim H}$ angle (label 8) of the dissociated structure ($NS_{DIS}$) is clearly above the 90° threshold by Langel and Parrinello [29] the dissociation would appear favorable in contrast to the $NP_{DIS}$ model. At 102°, the corresponding parameter for MgO is well above the threshold [30]. Consequently, water dissociation is also favorable at the MgO step. This value is considerably higher than the 90° calculated for the MgO step by Langel and Parrinello [29]. The proposed transfer of the hydrogen fragment from water to the NiO surface can be seen by the different $R_{NiO\sim H}$ and $R_{O\sim H}$ values in Table 4 (labels 2 and 4,

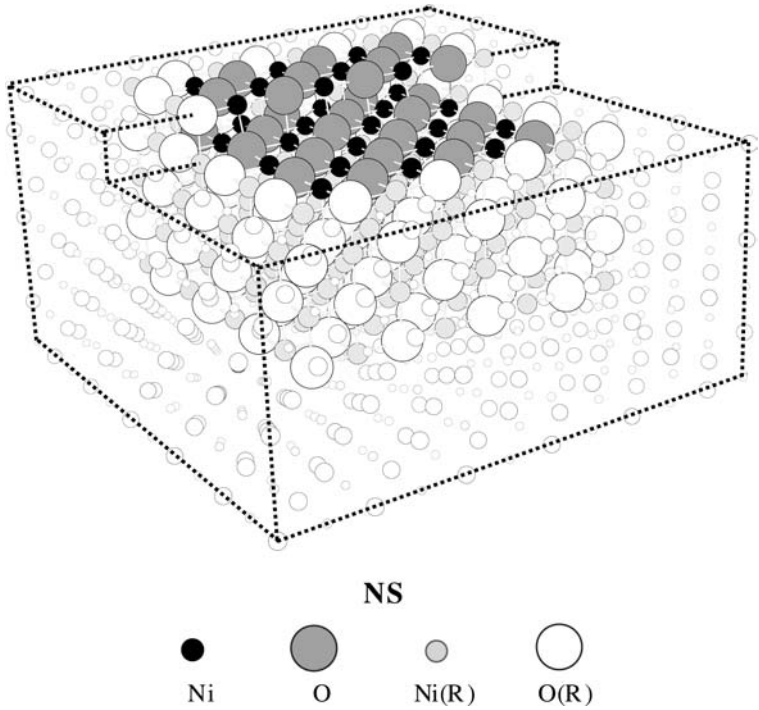


**Fig. 4** The embedded 8×8×4+8×4×1 NiO cluster with 6×6×1+6×3×1 relaxation (NS) representing the monatomic step region: relaxed nickel and oxygen atoms denoted Ni and O, respectively while fixed nickel and oxygen atoms denoted Ni(R) and O(R), respectively

**Table 4** Calculated bond lengths $R_{Ni-OH}$, $R_{NiO\sim H}$, $R_{Ni-O}$, $R_{O\sim H}$ and $R_{O\cdot O}$ (Å), and bond angles $\Phi_{H-O\sim H}$, $\Phi_{O\sim H\sim O}$ and $\Phi_{Ni-O\sim H}$ (degrees) for molecular and dissociated structures based on NS model with 6×6×1+6×3×1 relaxation (as shown in Fig. 5). Adsorption energies are denoted by $E_{ads}$ (kJ mol$^{-1}$); see Eq. (2). Results based on equivalent MgO models in parenthesis [30]

| Model | Label No. | NS | $NS_{MOL}$ | $NS_{DIS}$ |
|---|---|---|---|---|
| $R_{Ni-OH}$ | 1 | | 2.17 | 1.92 |
| $R_{NiO\sim H}$ | 2 | | 2.00 | 0.96 |
| $R_{Ni-O}$ | 3 | 2.07 (2.10) | 2.21 (2.17) | 2.56 (2.95) |
| $R_{O\sim H}$ | 4 | | 0.99 | 2.20 |
| $R_{O\cdot O}$ | 5 | | 2.59 (2.76) | 2.84 (2.85) |
| $\Phi_{H-O\sim H}$ | 6 | | 108 | 134 |
| $\Phi_{O\sim H\sim O}$ (ave.) | 7 | | 108 (106) | 103 (109) |
| $\Phi_{Ni-O\sim H}$ (ave.) | 8 | | 95 (96) | 93 (102) |
| $E_{ads}$ | | | −113 (−116) | −190 (−240) |

**Table 5** Calculated bond lengths $R_{Ni-OH}$, $R_{NiO\sim H}$, $R_{Ni-O}$, $R_{O\sim H}$ and $R_{O\cdot O}$ (Å), and bond angles $\Phi_{H-O\sim H}$, $\Phi_{O\sim H\sim O}$ and $\Phi_{Ni-O\sim H}$ (degrees) for molecular, transition state and dissociated structures based on NS model with 2×1×1+2×1×1 relaxation (as shown in Fig. 6). Adsorption energies are denoted by $E_{ads}$ (kJ mol$^{-1}$); see Eq. (2). Results based on equivalent MgO models in parenthesis [30]

| Model | Label No. | NS(R) | $NS_{MOL}$(R) | $NS_{TS}$(R) | $NS_{DIS}$(R) |
|---|---|---|---|---|---|
| $R_{Ni-OH}$ | 1 | | 2.13 | 2.00 | 1.92 |
| $R_{NiO\sim H}$ | 2 | | 1.94 | 1.41 | 0.97 |
| $R_{Ni-O}$ | 3 | 2.24 (2.40) | 2.31 (2.47) | 2.24 (2.59) | 2.33 (2.95) |
| $R_{O\sim H}$ | 4 | | 0.99 | 1.15 | 2.04 |
| $R_{O\cdot O}$ | 5 | | 2.57 (2.71) | 2.37 (2.49) | 2.68 (2.66) |
| $\Phi_{H-O\sim H}$ | 6 | | 108 | 116 | 136 |
| $\Phi_{O\sim H\sim O}$ (ave.) | 7 | | 108 (108) | 120 (119) | 102 (109) |
| $\Phi_{Ni-O\sim H}$ (ave.) | 8 | | 96 (97) | 90 (101) | 92 (102) |
| $E_{ads}$ | | | −98 (−99) | −24 (−82) | −168 (−206) |

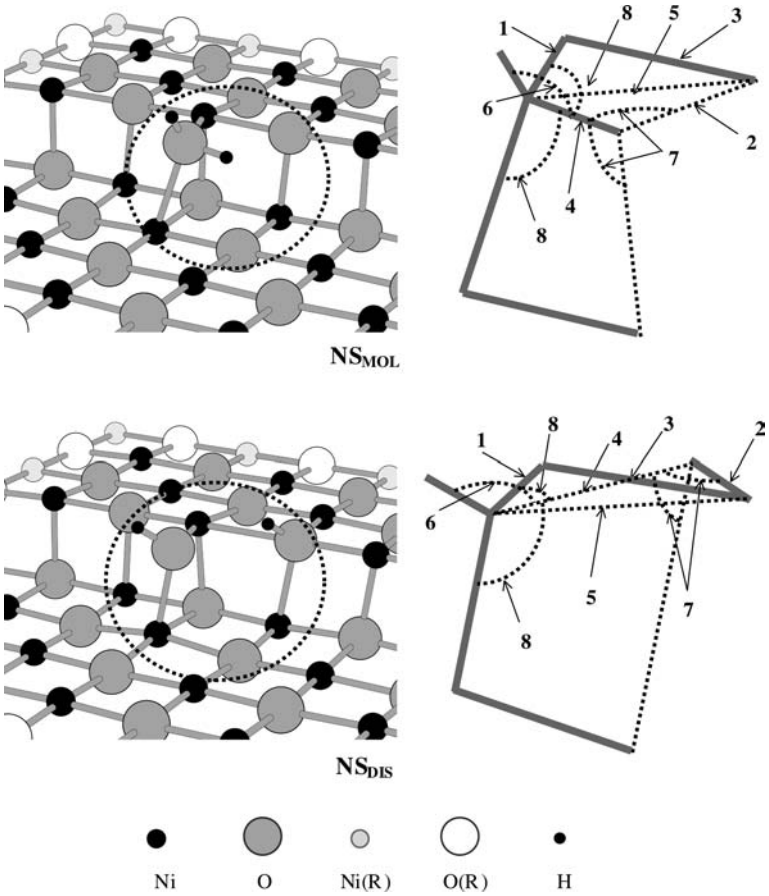


**Fig. 5** Molecular and dissociative adsorption for single water molecule on the stepped NiO surface with 6×6×1+6×3×1 relaxation: selected distances and bond angles highlighted by lines are labeled 1–8: (1) $R_{Ni-OH}$, (2) $R_{NiO\sim H}$, (3) $R_{Ni-O}$, (4) $R_{O\sim H}$, (5) $R_{O\cdot\cdot O}$, (6) $\Phi_{H-O\sim H}$, (7) $\Phi_{O\sim H\sim O}$ and (8) $\Phi_{Ni-O\sim H}$

respectively) for $NS_{MOL}$ and $NS_{DIS}$. The dissociative adsorption of water increases the $R_{Ni-O}$ bond length (label 3) of the adsorption site by 24% with respect to the dry surface NP. This increase is considerably larger than for the dissociative adsorption on the planar surface. Therefore, dissociative adsorption has a marked effect on the bond strength between atoms of reduced coordination. With an increase of 40%, this effect is even more pronounced for the MgO step [30].

Based on Eq. (2), the adsorption energy was calculated with respect to gas phase water.

$$Ni_{144}O_{144} + H_2O \rightarrow [Ni_{144}O_{144} : H_2O] \quad (2)$$

The adsorption energies for molecular and dissociative adsorption (Table 4) with 6×6×1+6×3×1 relaxation are −113 and −190 kJ mol$^{-1}$, respectively. Molecular adsorption at the monatomic step is considerably more exothermic compared to adsorption at the planar surface. The corresponding values for MgO are −116 and −240 kJ mol$^{-1}$, respectively [30]. The adsorption energies for molecular adsorption at the step sites are almost the same for both oxides. In the case of the MgO step, the calculated adsorption energy is much larger than the −65 kJ mol$^{-1}$ calculated by Langel and Parrinello [29]. Besides the differences in the underlying theoretical methods, the reason for the large difference is likely due to differences in the coordination number of the adsorption sites. As mentioned before, they use only five fold coordinated sites while our models contain four fold coordinated sites.

### 4.2 Models with 2 × 1 × 1 + 2 × 1 × 1 relaxation

Similarly as for the planar surface, we used a smaller number of surface atoms for the optimization of transition structures. In the restricted models, two atoms at the step and two atoms in the layer below the step were optimized (2×1×1+2×1×1 relaxation).

The restricted surface models representing molecular and dissociated adsorption in Fig. 6 are denoted $NS_{MOL}$(R) and $NS_{DIS}$(R), respectively. In addition, the transition state structure with restricted surface is denoted $NS_{TS}$(R).

Unlike the planar surface, there are some significant geometrical differences between the 6×6×1+6×3×1 relaxed monatomic step and the step with restricted relaxation. Firstly, for the dry surface, the $R_{Ni-O}$ bond distance (label 3) is longer in the restricted model NS(R) with respect to NS. For

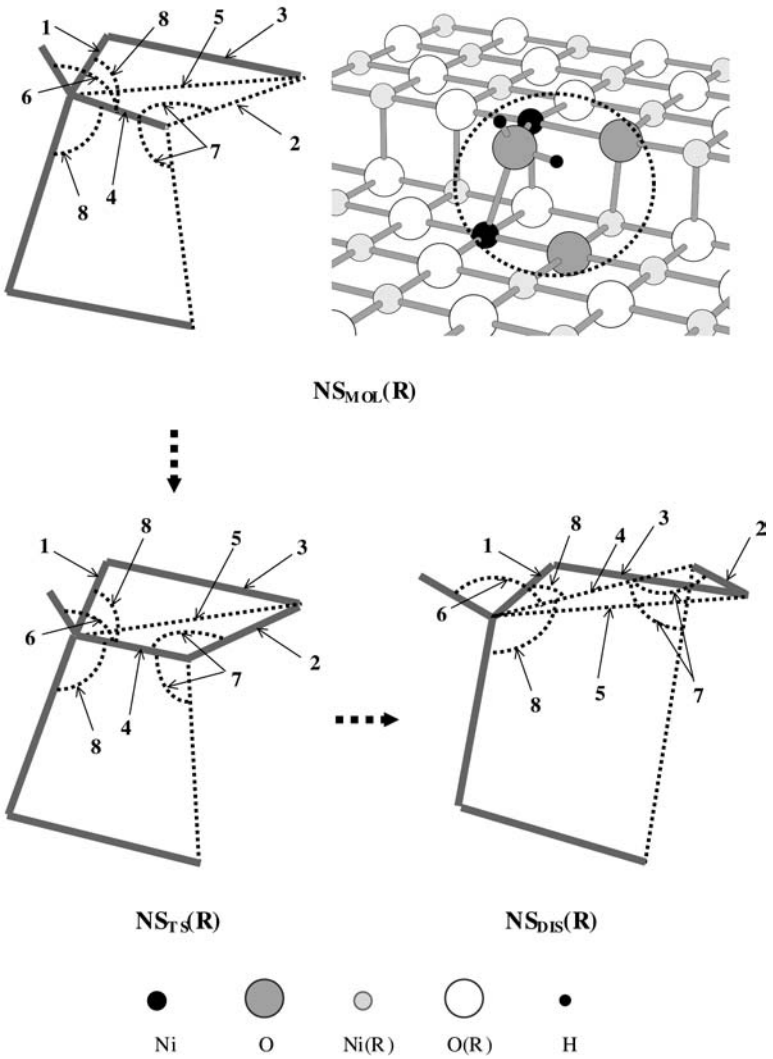


**Fig. 6** Adsorption of a single water molecule on the stepped NiO surface with $2\times1\times1$+$2\times1\times1$ relaxation for molecular, transition state and dissociative configurations: selected distances and bond angles highlighted by lines: (1) $R_{\mathrm{Ni-OH}}$, (2) $R_{\mathrm{NiO\sim H}}$, (3) $R_{\mathrm{Ni-O}}$, (4) $R_{\mathrm{O\sim H}}$, (5) $R_{\mathrm{O\cdot O}}$, (6) $\Phi_{\mathrm{H-O\sim H}}$, (7) $\Phi_{\mathrm{O\sim H\sim O}}$ and (8) $\Phi_{\mathrm{Ni-O\sim H}}$

molecular adsorption, the $R_{\mathrm{Ni-O}}$ bond of the surface in Table 5 is also significantly longer. Compared to $\mathrm{NS_{MOL}}$(Table 4), the shorter $R_{\mathrm{Ni-OH}}$ and $R_{\mathrm{NiO\sim H}}$ distances (labels 1 and 2, respectively) of $\mathrm{NS_{MOL}}$(R) (Table 5) indicate that the water molecule is adsorbed more closely to the surface after restricted optimization.

For dissociative adsorption, however, the $R_{\mathrm{Ni-O}}$ (label 1) bond length of $\mathrm{NS_{DIS}}$(R) is also reduced compared to $\mathrm{NS_{DIS}}$ (Table 4). There is also a marked reduction in the $R_{\mathrm{O\cdot\cdot O}}$ (label 5) parameter with relaxation area restriction. As for the planar surface, the $R_{\mathrm{Ni-O}}$ (label 3) bond distance of the transition state model is the same as the dry surface value. Similar to the planar NiO surface, the $R_{\mathrm{Ni-O}}$ bond length of the monatomic step is shortened with respect to the molecular structure in order to accommodate the transition state configuration. In contrast, there is a significant increase in the corresponding bond length of MgO [30]. The $\Phi_{\mathrm{Ni-O\sim H}}$ (label 8) angle of $\mathrm{NS_{TS}}$(R) is slightly smaller than corresponding values for $\mathrm{NS_{MOL}}$(R) and $\mathrm{NS_{DIS}}$(R). Although the rigidity of the NiO(100) surface forces the $\Phi_{\mathrm{Ni-O\sim H}}$ angle in structure $\mathrm{NS_{TS}}$(R) down to the 90° threshold, this value is clearly higher than the value $\Phi_{\mathrm{Ni-O\sim H}}$ of 64° calculated for the planar surface model. With the shortest $R_{\mathrm{O\cdot\cdot O}}$ distance (label 5) and largest $\Phi_{\mathrm{O\sim H\sim O}}$ angle (label 7) in Table 5, water in the transition state structure is more strongly hydrogen bound than water in the molecular and dissociated structures. The +74 kJ mol$^{-1}$ activation energy for the NiO step is much lower than the +198 kJ mol$^{-1}$ energy barrier calculated for the planar NiO surface and is comparable to the activation energy (+72 kJ mol$^{-1}$) for water dissociation on the planar MgO surface [30]. Based on this moderate activation energy, water dissociation is favorable considering the dissociated structure is +70 kJ mol$^{-1}$

more stable than the molecular structure. The same trend was also calculated for the equivalent MgO models. The only notable difference for MgO was the lower activation energy (+17 kJ mol$^{-1}$) and the $\Phi_{Mg-O\sim H}$ angle was 97, 101 and 102° for the molecular, transition state and dissociated structures, respectively [30]. These angles are well above the threshold for a successful reaction pathway.

## 5 Conclusions

From the numerous previous studies of water adsorption on surfaces with and without defects, there is a general consensus that water will dissociate at defect sites such as point defects and steps. This outcome was also obtained in the present MSINDO study. Water dissociation was found to be more favorable at the monatomic step compared to the planar surface. In addition, we have shown that water dissociation also depends on the chemistry of the surface. There are significant differences in the adsorption energies and geometrical parameters between isostructural (100) surfaces of NiO and MgO.

For molecular adsorption, the chosen size of the relaxation dimensions does not significantly affect the calculated adsorption energy, however, there is a strong dependence for dissociative adsorption. As mentioned before, the restricted models were chosen in this study due to the high computational demand of the transition state calculations. Apart from the effect on the adsorption energy of the dissociated structures, the geometrical measurements of the restricted models were reasonably close to corresponding values of the fully relaxed structures. Therefore, the limits imposed on surface optimization do not affect the outcome regarding the geometrical criteria.

As expected, adsorption at the monatomic step is more exothermic than the planar surface. The calculated activation energy for water dissociation is significantly lower in the monatomic step than on the planar surface. Molecular adsorption on the planar NiO surface is more exothermic than adsorption on the planar MgO surface. The activation energy for water dissociation was found to be higher at the NiO surface compared to equivalent MgO models.

Based on the geometrical criteria specified by Langel and Parrinello [29], water will dissociate at the stepped sites of both oxides. In contrast, water dissociation is highly improbable for the planar NiO surface. This is a consequence of the rigidity of the NiO structure preventing the water molecule from adopting a stable transition state; thereby creating a high activation energy. In accordance with the literature, water dissociation appears to be limited to NiO surfaces with defects such a monatomic steps. Dissociation of water on the planar MgO surface is a borderline case, but geometrical criteria tend to lean towards dissociation. It would seem reasonable that water dissociation on the planar MgO surface is reversible as suggested by Henderson [2].

**Acknowledgements** One of us (T.B.) gratefully acknowledges the Australian Research Council for an International Research Fellowship. The calculations were carried out on a SG Power Challenge at University of Adelaide. The structure drawings were created with Moviemol [33].

## References

1. Stumm W (1992) In: Chemistry of the solid-water interface. Wiley, New York
2. Henderson MA (2002) Surf Sci Rep 46:1
3. Schulze M, Reissner R (2001) Surf Sci 482–485:285
4. Henrich VE (1993) Springer Ser Surf Sci 33:125
5. Sanders HE, Gardner P, King DA, Morris MA (1994) Surf Sci 304:159
6. Rohr F, Wirth K, Libuda J, Cappus D, Baeumer M, Freund HJ (1994) Surf Sci 315:L977
7. Simpson DJ, Bredow T, Smart RStC, Gerson AR (2002) Surf Sci 516:134
8. de Leeuw NH, Parker SC (1998) Phys Rev B 58:13901
9. Segall RL, Smart RStC, Turner PS (1988) In: Nowotny J, Dufour LC (eds) Oxide surfaces in solution, in surface and near-surface chemistry of oxide materials. Elsevier, Amsterdam, pp 527–576
10. Simpson DJ (2003) Dissertation, University of South Australia
11. Ludwig C, Casey WH (1996) J Colloid Interface Sci 178:176
12. Jones CF, Segall RL, Smart RStC, Turner PS (1977) J Chem Soc Faraday Trans I 73:1710
13. Pease WR, Segall RL, Smart RStC, Turner PS (1986) J Chem Soc Faraday Trans I 82:759
14. Parks GA (1965) Chem Rev 65:177
15. Pople JA, Beveridge DL (1970) In: Approximate molecular orbital theory. McGaw-Hill, New York
16. Nanda DN, Jug K (1980) Theoret Chim Acta 57:95
17. Ahlswede B, Jug K (1999) J Comput Chem 20:563, ibid, 572
18. Zerner ML (1972) Mol Phys 23: 963
19. Bredow T, Geudtner G, Jug K (2001) J Comput Chem 22:861
20. Bredow T, Geudtner G, Jug K (2001) J Comput Chem 22:89
21. Schluff HP (1991) Dissertation, Universität Hannover
22. Geudtner G (1995) Dissertation, Universität Hannover
23. Bredow T, Geudtner G, Jug K (1996) J Chem Phys 105:6395
24. Ferry D, Picaud S, Hoang PNM, Girardet C, Giordano L, Demirdjian B, Suzanne J (1998) Surf Sci 409:101
25. Ahlswede B, Homann T, Jug K (2000) Surf Sci 445:49
26. Gerson AR, Bredow T (1999) Phys Chem Chem Phys 1:4889
27. Tikhomirov VA, Jug K (2000) J Phys Chem B 104:7619
28. Scamehorn CA, Harrison NM, McCarthy MI (1994) J Chem Phys 101:1547
29. Tikhomirov VA, Geudtner G, Jug K (1999) J Mol Struct (THEOCHEM) 458:161
30. Langel W, Parrinello MJ (1995) Chem Phys 103:3240
31. Simpson DJ, unpublished results
32. Reissner R, Schulze M (2000) Surf Sci 454–456:183
33. Bredow T, Jug K (1995) Surf Sci 327:398
34. Hermansson K, Ojamäe L (1994) University of Uppsala, Institute of Chemistry. Report UUIC-B19-500